Magnetic and Mössbauer study of multiphase Fe-Zr amorphous powders obtained by high energy ball milling

2000 J. Phys.: Condens. Matter 12 3101

(http://iopscience.iop.org/0953-8984/12/13/318)

J. Phys.: Condens. Matter **12** (2000) 3101–3112. Printed in the UK PII: S0953-8984(00)06490-0

Magnetic and Mössbauer study of multiphase Fe–Zr amorphous powders obtained by high energy ball milling

R Pizarro†, J S Garitaonandia‡, F Plazaola†, J M Barandiarán† and J M Grenèche§

† Departamento Electricidad y Electrónica, Facultad de Ciencias, Universidad del País Vasco, Apartado 644, E-48080 Bilbao, Spain

‡ Departamento Física Aplicada II, Facultad de Ciencias, Universidad del Pais Vasco, Apartado 644, E-48080 Bilbao, Spain

§ Laboratoire de Physique de L'Etat Condensé, UPRES A CNRS 6087, Université du Maine, 72085 Le Mans Cédex 9, France

Received 30 July 1999, in final form 15 December 1999

Abstract. The amorphous system Fe–Zr has been extensively studied due to its particular magnetic behaviour, especially in the concentration range around 90 at.% Fe, only accessible by rapid quenching. We have extended the study to lower Fe content alloys, by using mechanical alloying to synthesize Fe_xZr_{100-x} amorphous powders with $x = 65, 70, 75$. Mössbauer spectra and magnetization measurements have been performed as a function of temperature. Different magnetic measurements were performed to characterize the Curie temperatures of these multiphase samples and hyperfine field (B_{hf}) distributions, $P(B_{hf})$, were used to fit Mössbauer spectra below the Curie temperature (T_C) and quadrupole splitting distributions, $P(\Delta)$, above T_C, in agreement with the amorphous structures. The hyperfine field distributions of as-milled samples are characterized by two maxima and are fitted with two Gaussian curves that evolve with temperature in position, intensity and width. This bimodal behaviour has been also found in higher Fe content FeZr alloys as well as in ternary alloys with boron, and with nickel, and can be interpreted as arising from different neighbourhood Fe sites. The rather uncommon $P(\Delta)$ are also interpreted in the same terms.

1. Introduction

Amorphous Fe–Zr alloys have been extensively studied in the last 20 years and their complex magnetic behaviour has been a subject of intensive experimental and theoretical research. Indeed, Fe rich alloys, usually rapid quenched ribbons, show interesting anomalous magnetic phenomena at low temperature such as Invar and re-entrant spin-glass behaviour [1–4]. In addition, some electronic structure calculations have predicted the distribution of magnetic moments, the non-collinear magnetic arrangement and the spin-glass ordering. But it is important to emphasize that the magnetic properties of amorphous Fe–Zr alloys are strongly dependent on Fe content and on the local atomic order.

For iron content below 90 at.%, rapid quenching technique from the molten state is not able to produce the amorphous alloy, except for concentrations around 25 at.% Fe, which is not magnetically interesting. So, other methods have to be used to produce the amorphous phase, such as the sputtering technique [4, 5] or mechanical alloying [6, 7]. For example, by the mechanical alloying technique amorphous samples can be obtained in the range 30–78 at.% Fe [6]. Indeed, the principles of these routes favour the synthesis of atomic scale disordered alloys either coated on a substrate or in fine powders, respectively. For these concentrations

0953-8984/00/133101+12$30.00

the system has at least two transformations as a function of concentration, that is from superconductor below ≈30 at.% Fe to paramagnetic, and to ferromagnetic above ≈45 at.% Fe [4]. Nevertheless, there are no many exhaustive magnetic and structural studies for these alloys in the ferromagnetic region below 90 at.% Fe.

The aim of this work is twofold: (a) to synthesize FeZr amorphous ferromagnetic powders below the Fe composition range obtained by the melt spinning technique and (b) to study the structural and magnetic homogeneity of the thus obtained amorphous samples. In that way, the amorphous alloys Fe_xZr_{100-x} with $x = 65, 70, 75$ have been synthesized by means of high energy ball milling, so-called mechanical alloying, that allows us to obtain the amorphous phase in a wide concentration range [6–9] and provides a considerable amount of powdered sample. The amorphous samples were characterized by means of x-ray diffraction, magnetic measurements and ^{57}Fe Mössbauer spectrometry, so that we obtained information about the global magnetic behaviour as well as about the local structure, at zero applied field, as a function of temperature.

2. Experimental section

Pure Fe and Zr powders (99.99%) were milled under Ar atmosphere in a Retsch PM 4 planetary ball mill with a nominal concentration of Fe_xZr_{100-x} ($x = 65, 70, 75$). All the samples were milled at the same mill operation velocity of 300 r.p.m., in Cr steel vials. The ball diameter was 10 mm, and powder to balls mass ratio was fixed to 1:10. In order to check the evolution of the amorphicity of the samples two techniques were used: x-ray diffraction (Cu-Kα radiation was used) and ^{57}Fe Mössbauer spectrometry. The isomer shift values are quoted relative to that of bcc-Fe at 300 K. The x-ray diffraction patterns are presented in Figure 1 corresponding to 35 milling hours for $x = 65, 75$ samples and 45 milling hours for the $x = 70$ sample. A good amorphous state was presumed, although a small reflection around $2\theta = 32^\circ$ indicates that there is a minimum quantity of non-amorphous pure Zr without any influence on the magnetic response of the samples. Besides, a small contribution (in all cases less than 2 at.%) which is unambiguously attributed to α-Fe was only observed on low temperature Mössbauer spectra (see below) because the magnetic hyperfine structure favours the occurrence of small satellite lines in contrast to RT where the absorption is contained in the quadrupolar doublet.

Magnetic characterization was done using a Quantum Design SQUID magnetometer. Magnetization–field and low field magnetization–temperature measurements were performed

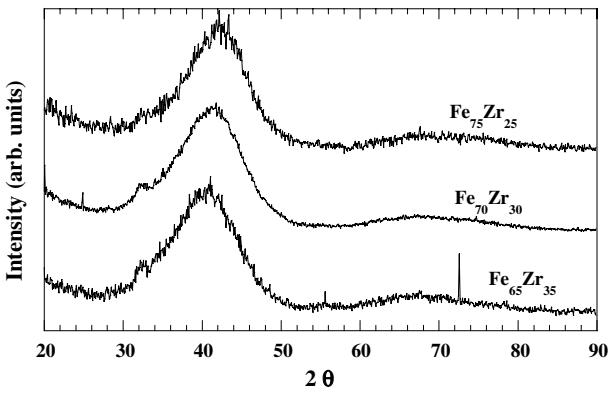

Figure 1. X-ray diffraction patterns of the as-milled $Fe_{65}Zr_{35}$, $Fe_{70}Zr_{30}$ and $Fe_{75}Zr_{25}$ samples.

to obtain both the saturation magnetization and the Curie temperatures (T_C) as well as to check the chemical and structural homogeneity of the alloys looking at the fall of the magnetization around T_C.

Transmission Mössbauer spectra were measured using a conventional constant acceleration spectrometer as a function of temperature, between 4 K and room temperature (RT). Experimental Mössbauer spectra were fitted with Brand's NORMOS program [10] and with the MOSFIT program developed by Teillet and Varret [11] using two components below the amorphous Curie temperature (T_C): one crystalline magnetic sextet for crystalline α-Fe, when present, and a distribution of hyperfine fields ($P(B_{hf})$) to describe the sextet with broadened and overlapped lines assigned to the amorphous phase. Above T_C, the quadrupolar doublets with broad lines are reproduced with distributions of quadrupole splitting, $P(\Delta)$. Linear correlations between $P(B_{hf})$ and the isomer shift distribution P(IS) below T_C and different types of correlation between $P(\Delta)$ and P(IS) were included to account for the asymmetry of the spectra above T_C, respectively. Then, the resulting $P(B_{hf})$ were fitted at each temperature with two independent Gaussian curves while $P(\Delta)$ were compared to those predicted by different structural models.

3. Results and discussion

3.1. Magnetic measurements

Low temperature magnetization (figure 2(a)) and thermomagnetic curves at 200 or 300 Oe applied field (figure 2(b)) were recorded for the as-milled samples. These fields are high enough to overcome the coercivity but low enough to give a sharp magnetic transition at T_C. Magnetic saturation is reached in relatively low fields and the magnetic moment per iron atom can be easily obtained. The relatively sharp decrease in M at the Curie temperature, T_C, allows us to estimate it as the minimum of $\mathrm{d}M/\mathrm{d}T$. The temperature range at which $\mathrm{d}M/\mathrm{d}T$ deviates from zero is large. Such a feature might be consistent with a somewhat distributed transition that can arise from composition inhomogeneities, due to the milling process. It is important to emphasize that T_C is strongly dependent on the Fe content within this concentration range in the case of the FeZr system. So, one concludes the presence of composition inhomogeneities.

The increase of both T_C and M_s (5 K) (table 1) with Fe enrichment is in agreement with previously published results for this system within the same concentration range [4], and its values allow us to confirm that the present as-milled amorphous phases are near nominal average concentration.

Complementary to these measurements, modified Arrot plots [12] were made on the $Fe_{75}Zr_{25}$ sample. Arrot plots are known to be very sensitive to magnetic inhomogeneities [13] and they can give insight into the concentration spread in these compounds. Magnetization versus applied field between 0.5 and 4 T was measured with a field increase of 0.5 T in the temperature range 180–300 K. Although the linear fit is not perfect in the vicinity of magnetic transition, the critical exponents β and γ were estimated at 0.35 and 1.36, respectively. These values are in good agreement with those found in FeZrB alloys prepared by rapid quenching [14]. In figure 3 are represented $M_s^{1/\beta}$ versus $(H/M)^{1/\gamma}$ (a) and $M_s^{1/\beta}$ versus temperature ($T < T_C$) and inverse susceptibility versus temperature ($T > T_C$) (b) for the as-milled sample $Fe_{75}Zr_{25}$. The static magnetic measurements reveal different ferromagnetic Curie temperatures (extrapolated from $T < T_C$) about 15 K less than in the previous measurement. It seems that Arrot plots give the lowest value of T_C while $\mathrm{d}M/\mathrm{d}T$ indicates the most probable one in a distribution. Such a feature suggests the presence of some magnetic inhomogeneity in the

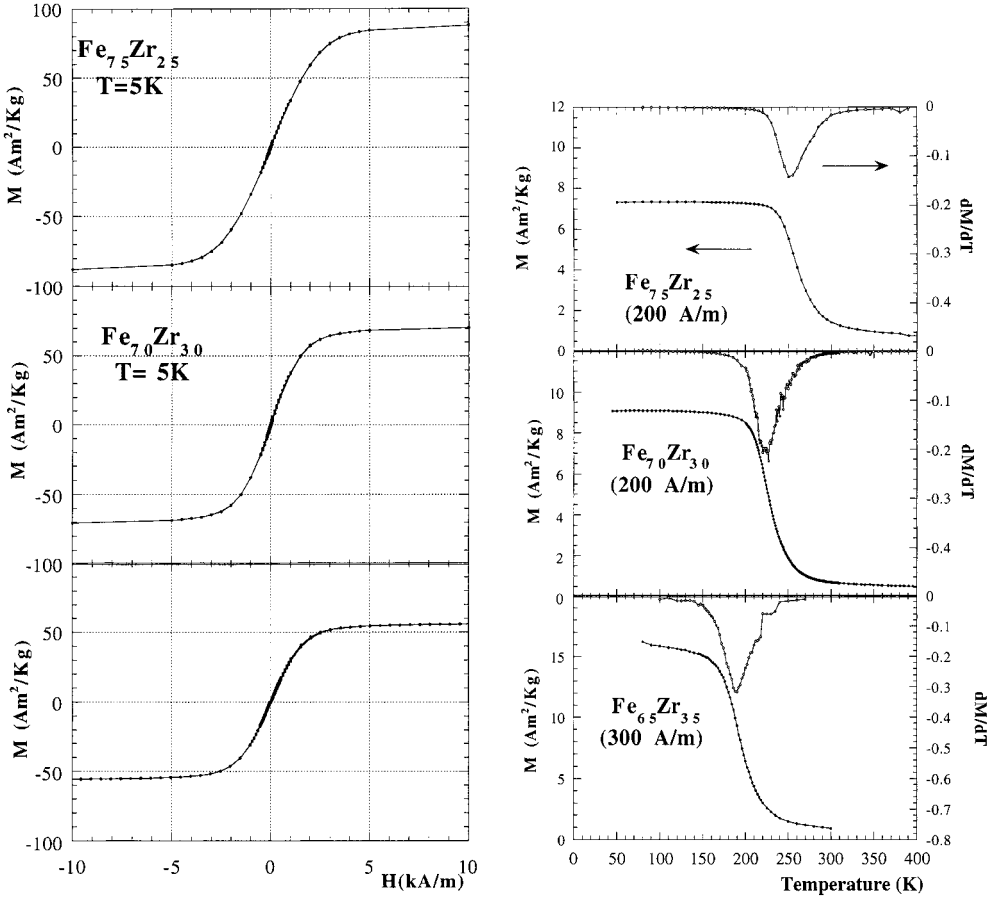

(a) (b)

Figure 2. (a) Magnetization curves taken at 5 K for the different as-milled $Fe_{75}Zr_{25}$, $Fe_{70}Zr_{30}$ and $Fe_{65}Zr_{35}$ samples. (b) Thermomagnetic curves at 200 or 300 A m^{-1} applied field. The minima of dM/dT are taken as the mean T_C of the samples.

Table 1. Magnetic parameters of the samples. The Curie temperatures have been deduced from the magnetization derivative against temperature. The M_s and μ_{Fe} values present an error of 1%; the error for the Curie temperatures is ±2 K.

Sample	M_s (5 K) (A m^2 kg^{-1})	μ_{Fe} (5 K) (μ_B)	T_C (K) (dM/dT)
$Fe_{65}Zr_{35}$	55	1.03	190
$Fe_{70}Zr_{30}$	70	1.19	220
$Fe_{75}Zr_{25}^{a}$	89/95[a]	1.38	252/270

[a] As milled/annealed 500 °C, 1 h.

samples. The paramagnetic Curie temperature (extrapolated from $T > T_C$) is also different from the ferromagnetic one, but this can arise from the itinerant character of the ferromagnetism in these samples.

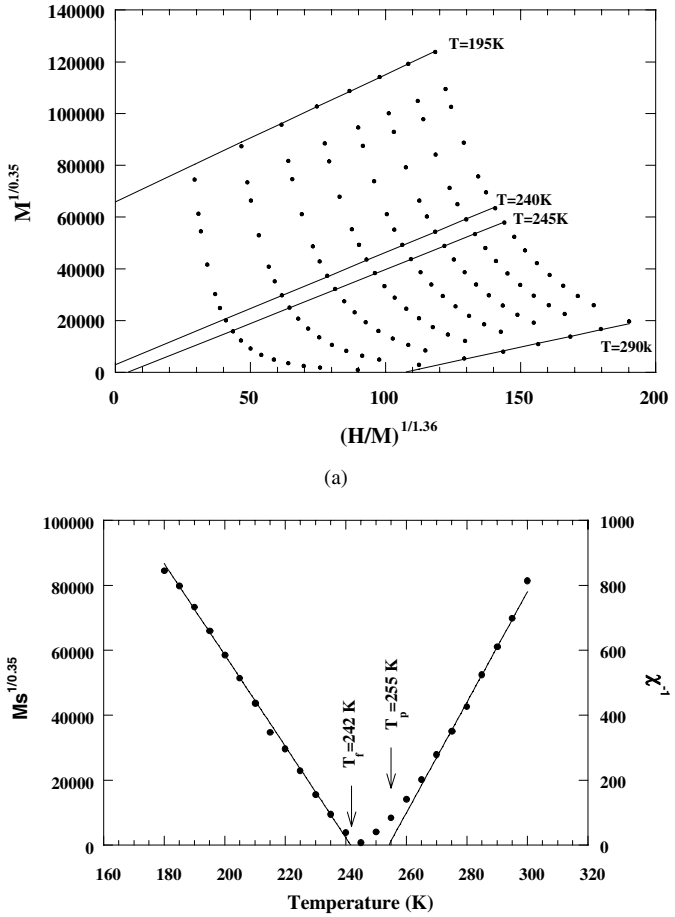

Figure 3. Modified Arrot plot (a) as well as spontaneous magnetization (M_s) with inverse susceptibility versus temperature (b), for the sample $Fe_{75}Zr_{25}$ as milled.

3.2. Mössbauer spectrometry

Some Mössbauer spectra above and below T_C are shown in figures 4 and 5 for as-milled samples. The room temperature spectra exhibit unresolved asymmetrical quadrupolar structures as usually observed in the case of as-quenched amorphous alloys. It is important to note that neither a pure Δ discrete distribution, $P(\Delta)$, nor linearly correlated $P(\Delta)$ and $P(\mathrm{IS})$ models were able to properly describe the quadrupolar spectra of the present as-milled FeZr powders, in contrast to most as-quenched amorphous alloys, particularly FeZr alloys. The best fits which are reported there [1, 4] were obtained using uncorrelated $P(\Delta)$ and $P(\mathrm{IS})$, where IS values are slightly dispersed. Nevertheless, a fitting procedure based on the superimposition of two subcomponents, each one resulting from linearly correlated $P(\Delta)$ and $P(\mathrm{IS})$ with negative and positive correlation coefficients, in agreement with subspectra of opposite asymmetry, can be applied. This procedure is physically realistic but *a priori* rather complex due to the strong overlap. But it was successfully applied on the paramagnetic spectra and those results were considered below. This model remains consistent with a non-homogeneous local structure

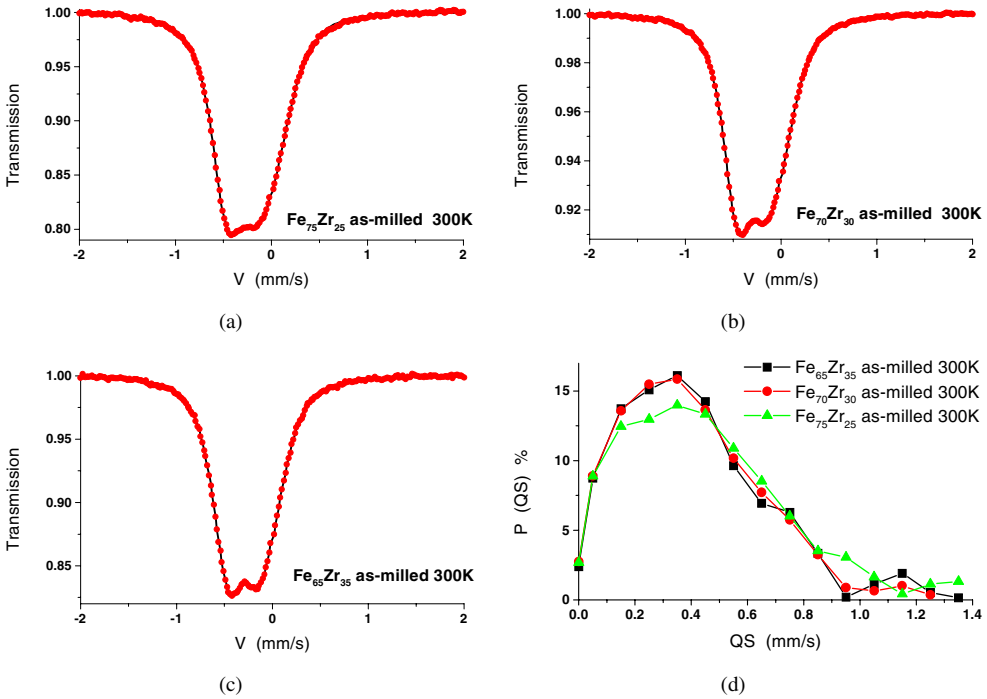

Figure 4. Mössbauer spectra at room temperature and the corresponding quadrupole splitting distributions for as-milled $Fe_{75}Zr_{25}$, $Fe_{70}Zr_{30}$ and $Fe_{65}Zr_{35}$ samples.

and the existence of two different Fe local environments. Indeed, the different isomer shift values that reflect the s density at Fe nuclei can be interpreted in terms of local free volume of Fe environments whereas the quadrupolar splitting reflects the asymmetry of the structural environments. The present results might be consistent with different local Fe environments with different densities.

It is also important to emphasize that $P(\Delta)$ shows, as a special feature, a non-zero contribution at zero Δ whatever the fitting model is. This distribution is rather unusual but has been already reported in the case of ball milled FeZr alloys, without further discussion [15]. From the point of view of the local structure, Fe atoms having zero Δ have to be located in an highly symmetrical site. As observed in figure 4, their proportion significantly differs from zero, that remains difficult to understand in an amorphous state. This contribution could be attributed to the occurrence of small crystalline iron clusters which remain after the milling process.

The usual Δ distributions found in most amorphous solids are in good agreement with those predicted by the random packing of hard spheres model, proposed by Czjzek *et al* [16] and recently discussed in a review paper [17]. The Δ distributions are generally expressed as:

$$P(\Delta) = (1/\sigma^n)\Delta^{n-1}\exp(-\Delta^2/2\sigma^2). \tag{1}$$

Here n (generally comprised between 2 and 5) represents a parameter which gives the dimensionally of the local probe unit or, to put it better, the kind of local anisotropy. A random hard spheres model for a disordered solid has $n = 5$. Much lower values, like $n = 2$, were found for amorphous FeF_3, the structure of which can be described as a random packing of octahedral units [18, 19]. In our case, the only possibility is to use a value intermediate

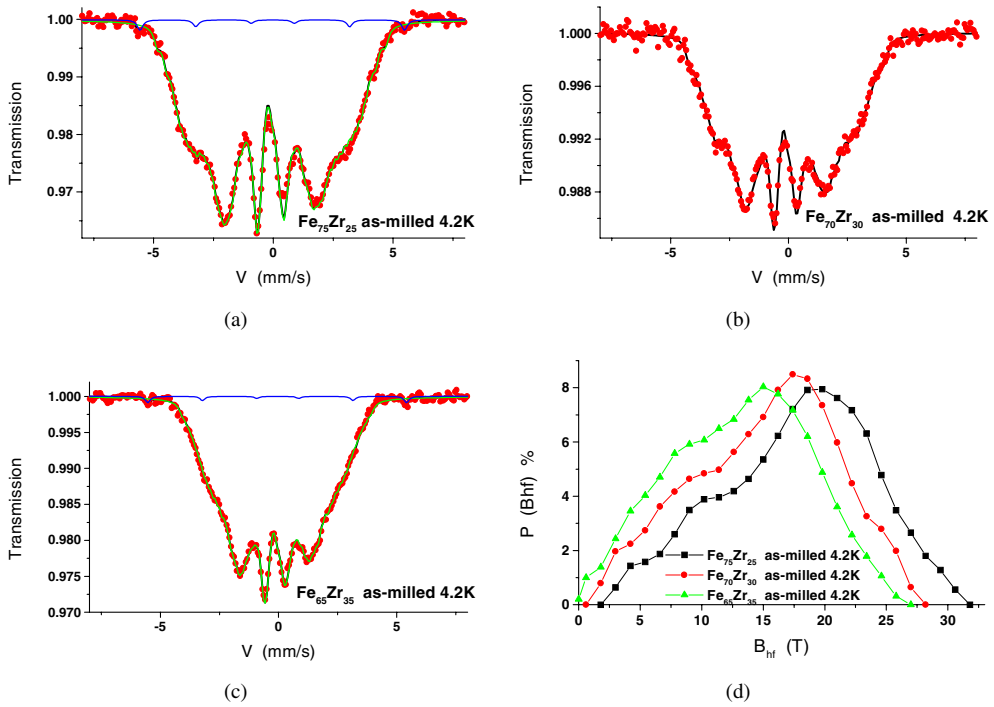

Figure 5. Mössbauer spectra at 4.2 K and the corresponding hyperfine field distributions for as-milled $Fe_{75}Zr_{25}$, $Fe_{70}Zr_{30}$ and $Fe_{65}Zr_{35}$ samples.

Table 2. Mössbauer parameters of the as-milled samples in the paramagnetic (room temperature) and ordered (77 K) states. The isomer shift (IS) is taken with respect to an α-Fe calibration foil measured at room temperature. All the values are given with a 1% error.

Sample	$\langle IS\rangle$ (RT) (mm s^{-1})	$\langle\Delta\rangle$ (RT) (mm s^{-1})	$q = \langle\Delta^2\rangle/\langle\Delta\rangle^2$	$\langle IS\rangle$ (77 K/4 K) (mm s^{-1})	$\langle B_{hf}\rangle$ (77 K/4 K) (T)
$Fe_{65}Zr_{35}$	−0.16	0.40	1.41	−0.02/ − 0.01	10.8/12.9
$Fe_{70}Zr_{30}$	−0.13	0.39	1.39	0.00/0.01	13.2/15.1
$Fe_{75}Zr_{25}$	−0.12	0.43	1.42	−0.01/0.00	15.2/17.2

between 1 and 2, if the value of $P(\Delta = 0)$ is to be accounted for. This is also indicated by the values of the parameter q:

$$q = \langle\Delta^2\rangle/\langle\Delta\rangle^2. \tag{2}$$

The expected values of q increase from 1.1 , corresponding to $n = 5$, to 1.27 for $n = 2$, as observed in numerous amorphous ferric fluorides. In our case q takes a value around 1.4 for all the samples (see table 2). This corresponds to $n \approx 1.37$, and it is possible that, in fact, there was a distribution of n values because there is very difficult to fit the actual $P(\Delta)$ to any definite Czjzek distribution as given by (1). The simplest assumption, however, will be a combination of two different sites with $n = 1$ and $n = 2$, that can be ascribed to low coordination iron units.

As illustrated in figure 5, all samples are magnetically ordered at 4.2 K and the corresponding Mössbauer spectra exhibit broadened and overlapped lines. They can be fitted with a distribution of B_{hf} and, eventually, a sextet corresponding to some α-Fe not

yet amorphized. A linear correlation between B_{hf} and IS has been included to account for the asymmetry of the spectra [10]. The values of the correlation parameter are very similar in all samples and remain positive, i.e. the isomer shift increases with the hyperfine field. $P(B_{hf})$ reveals a bimodal behaviour with different positions and intensities depending on the composition and temperature, but very similar in any case (see figure 5). These $P(B_{hf})$ distributions give insight into a two site Fe structure, as already suggested from the quadrupole distributions. The low field values are ascribed to Zr-rich surroundings of Fe atoms whereas the low isomer shift values can be attributed to significantly reduced local volume. Finally, the average $\langle B_{hf} \rangle$ at 4.2 K scale with the magnetic moment per Fe atom with a constant of 12.5 T μ_B^{-1}, as has been found in a large variety of amorphous ferromagnetic materials [20].

In order to go farther in the description of the local structure of Fe, the evolution of the Mössbauer spectra has been followed as a function of temperature. The results are shown in figure 6 for $Fe_{75}Zr_{25}$. Similar results were found for other compositions.

The corresponding hyperfine field distributions $P(B_{hf})$ were successfully fitted with two Gaussian contributions, whatever the composition is. Only at low temperatures is there a low field component outside the curves, and its contribution is less than 2% of the total. Such a decomposition of $P(B_{hf})$, after fitting of the spectra, is possible because all alloys exhibit very similar IS values within the compositional range studied (see table 2). After the decomposition, the description of the magnetic state of the sample is described in terms of the relative intensity of both components, the position of the maximum (i.e. the average B_{hf}) and the standard deviation of each one.

These bimodal distributions of B_{hf} which have been previously observed in other systems [21] as well as in Fe–Zr alloys prepared with other techniques [1, 4], have been interpreted as resulting from magnetic clusters, either ferromagnetic or antiferromagnetic [1]. But they can be interpreted also as arising from different Fe sites in an otherwise homogeneous alloy. In any case the temperature evolution of the different contributions to $P(B_{hf})$ can give a clue for the interpretation of the underlaying structural components.

In figure 6(b) is evident the evolution of both Gaussian components with temperature. The contribution of the low field one grows as the temperature increases, while the high field one decreases. For $T > T_C$ (T_C determined from magnetic measurements) a small contribution of the high field Gaussian is still present and only disappears at about $T_C + 20$ K. Above this temperature hyperfine field distributions have no physical meaning because the system is totally in the paramagnetic state, and $P(\Delta)$ should be used instead, but it allows us to fix a base line for the Gaussian contributions and can be useful in the discussion. Figure 7(a) shows the temperature evolution of the maxima of the two Gaussian components. It should be noticed that the mean value of both contributions reaches a constant value at the same temperature, which is, however, 20 K below the expected T_C. The low field contribution which reaches a value below 2 T, i.e. equivalent to a Δ value of 0.65 mm s^{-1}, is assigned to Fe moments which are still in the paramagnetic state. However the high field contribution which remains at a rather high value of 7 T, is indicative of a ferromagnetic behaviour. Figure 7(b) shows the variation with temperature of the contribution of each Gaussian component to the total area of $P(B_{hf})$. The decrease of the high field component is slow until 230 K, and then falls down very quickly. At 230 K the high field contribution is still about 70% of the total, while the low field contribution has reached the paramagnetic domain. Spectra obtained in the temperature range 230–270 K were also fitted using a combination of a pure magnetic component (with free parameters during the fitting procedure) and a pure paramagnetic doublet (as obtained in the complete paramagnetic range). Such a procedure allows the paramagnetic fraction and its temperature dependence to be estimated, both being in agreement with data resulting from the previous model.

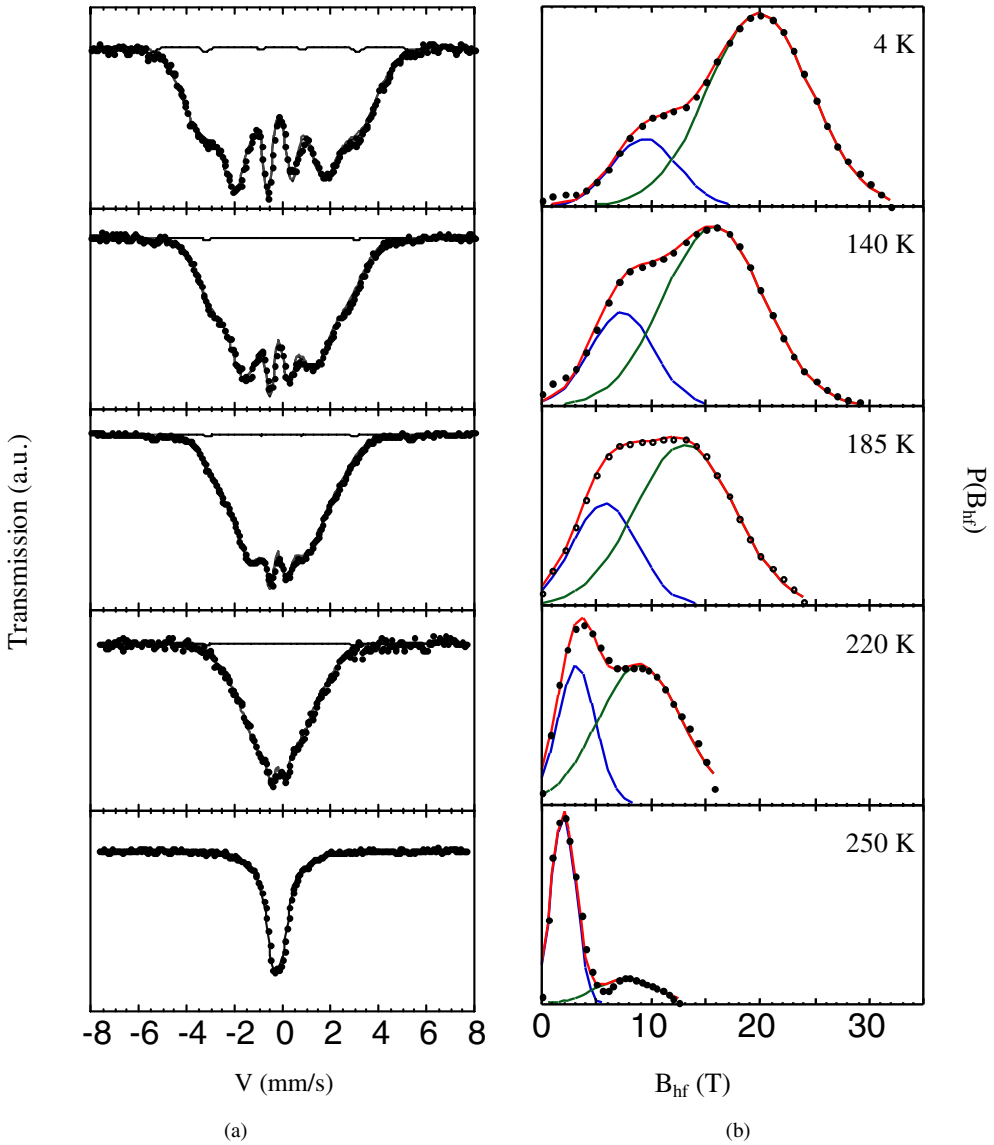

Figure 6. (a) Mössbauer spectra at various temperatures below T_C. (b) Corresponding hyperfine field distributions (dots) and two Gaussian fit (continuous lines), as well as resultant curve fit for as-milled $Fe_{75}Zr_{25}$. Similar behaviour was found for other compositions. As can be observed the scales of the spectra are not the same and the resonant areas appear relative at each scale. This is the reason for the apparent progressive decrease of the α-Fe component in the figure.

The temperature dependence of each Gaussian component is different, which suggests the existence of (at least) two different iron phases instead of a single phase with two kinds of Fe site. The existence of large inhomogeneities is not surprising in mechanically alloyed materials, as the alloying process implies the interdiffusion of the components: one expects that Fe diffusing into Zr can give rise to Zr-rich zones, while the opposite will occur when Zr atoms diffuse into Fe crystals. A two phase description of these alloys can be done in

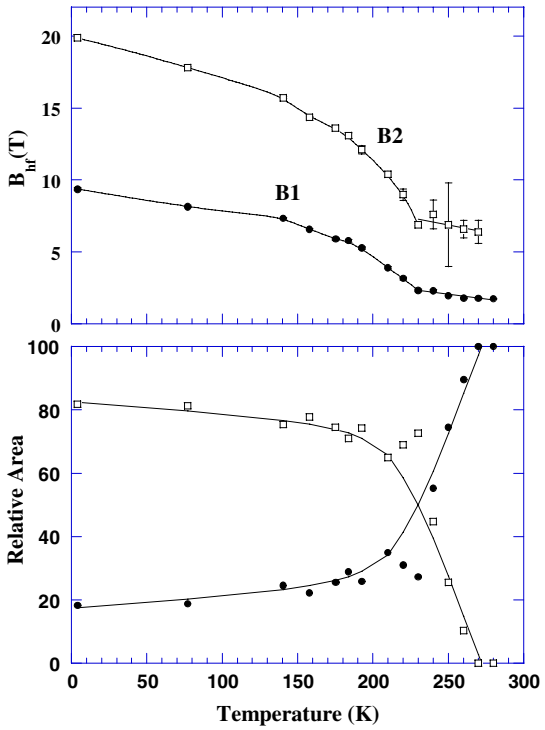

Figure 7. Evolution with temperature of (a) the average B_{hf} and (b) the relative area of each Gaussian component of $P(B_{hf})$ of the as-milled $Fe_{75}Zr_{25}$ sample.

terms of Fe-rich zones, with high T_C and high B_{hf}, on one side, and Zr-rich zones, with low T_C and low B_{hf}, on the other side. These different behaviours have been already observed in the as-quenched amorphous FeZr alloys [1, 2]. In those samples the different Gaussian components have been explained by means of local spin density fluctuations attributed to the existence of concentration fluctuations created during the sample preparation. Even thought the final structure of both kind of sample (as milled and as quenched) is very similar (both of them are amorphous with two different Fe regions), the preparation method appears to be crucial [22] to explain the different magnetic responses. In addition, the coercive field values of the as-milled samples are two orders of magnitude higher that those found in the literature for as-quenched samples [23]. Consequently, the different interdiffusion of the components in the milled samples is supported as an explanation for the different temperature evolutions of the Gaussian components.

3.3. Annealing and relaxation of the amorphous structure

In order to check the above assumptions, the $Fe_{75}Zr_{25}$ amorphous sample was annealed below the crystallization temperature (for 1 hour at 500 °C) under a controlled Ar atmosphere. As a result of such annealing treatment, an increase in the Curie temperature of about 20 K and a sharpening of the transition are clearly shown (figure 8). From the magnetic point of view, the effect of the annealing originates both the increase and the homogenization of the magnetic interactions.

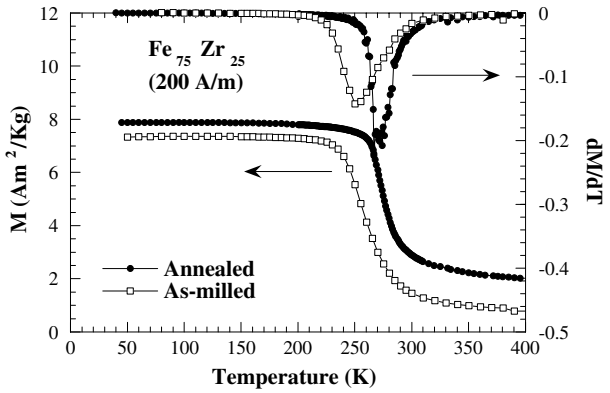

Figure 8. Evolution with temperature of the low field magnetization and its derivative for as-milled and annealed (1 h, 500 °C) $Fe_{75}Zr_{25}$ samples. Both an increase of T_C and a sharpening of the transition are evident.

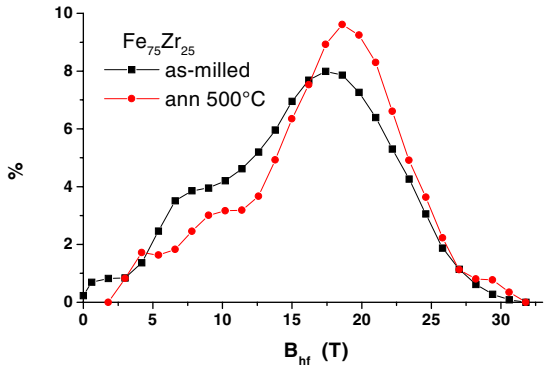

Figure 9. Hyperfine field distributions for as-milled and annealed (1 h, 500 °C) $Fe_{75}Zr_{25}$ samples at 77 K. The increase of $\langle B_{hf} \rangle$ is accompanied by a decrease of the low field contribution.

The increase of T_C, in this composition range, corresponds to a decrease of interatomic distances or to an increase of the Fe content: such a behaviour is opposite to that found in alloys with more than 85 at.% Fe [24, 25] because at these percentages the samples present Invar behaviour. The annealing treatment originates an increase from 1.3% to about 3% of the amount of free α-Fe, as estimated by Mössbauer spectroscopy. Thus, the amorphous component of the annealed sample presents a slight decrease of Fe content. This is confirmed by the increase in the magnetization remaining above the Curie temperature of the amorphous phase (see figure 8). Indeed, the increase of T_C observed after the annealing is due to the decrease of the interatomic process appearing as a consequence of the structural relaxation. Another consequence of the thermal treatment is the narrowing of the $M(T)$ derivative curve around the T_C temperature of the sample. As has been commented above, the shape of the derivative curves is intimately related to the homogeneity of the sample. In this sense, the observed narrowing indicates that the annealed sample is more chemically and structurally homogeneous that the as-milled precursor. The conclusion is that both the relaxation combined with the homogenization of the structure are responsible for this increase of the magnetic interactions.

The same conclusion is confirmed by Mössbauer experiments, essentially in the magnetic range. Figure 9 compares $P(B_{hf})$ taken at 77 K before and after the annealing treatment. The average hyperfine field is shifted to higher values and the low field contribution has decreased with respect to the high field one. In terms of the two phase description, that implies a redistribution of the Fe atoms into the Fe-poor and Fe-rich phases produced by further diffusion between the phases, together with a relaxation of each phase, that originates an increase of its magnetic moment, T_C and B_{hf}.

4. Conclusions

High energy ball milling allows amorphous FeZr alloys with Fe content comprised within the range 65–75 at.% to be successfully prepared. In addition to x-ray patterns which clearly provide evidence for amorphous structure, the hyperfine structure of both quadrupolar and magnetic Mössbauer spectra is consistent with the existence of two kinds of local environment. Zr-rich environments of Fe with reduced local volume are attributed to the low field component whereas the Fe-rich environments to the high field component.

The decomposition of hyperfine field distributions into two Gaussian components and their behaviour against temperature suggest that the two local environments correspond to two different Fe phases in the samples.

References

[1] Kaul S N, Siruguri V and Chandra G 1992 *Phys. Rev.* B **45** 12 343–56
[2] Ryan D H, Coey J M D, Batalla E, Altounian Z and Ström-Olsen J O 1997 *Phys. Rev.* B **35** 8630
[3] Vincze I, Kaptas D, Kemeny T, Kiss L F and Balogh J 1995 *J. Magn. Magn. Mater.* **140–144** 297
[4] Unruh K M and Chien C L 1984 *Phys. Rev.* B **30** 4968
[5] Krebs H U, Webb D J and Marshall A F 1987 *Phys. Rev.* B **35** 5392
[6] Schultz L and Eckert J 1994 *Topics in Applied Physics* vol 72 ed Beck and Guntherodt (Berlin: Springer)
[7] Burgio N, Iasonna A, Magini M and Padella F 1990 *J. Physique Coll.* **51** C4 265
[8] Hellstern E and Schultz L 1988 *J. Appl. Phys.* **63** 1408
[9] Michelsen C and Hellstern E 1987 *J. Appl. Phys.* **62** 117
[10] Brand R, Lauer J and Herlach D M 1984 *J. Phys. F: Met. Phys.* **14** 555
[11] Teillet J and Varret F MOSFIT program, University of Le Mans
[12] Arrot A 1957 *Phys. Rev.* B **108** 1394
[13] Aharoni A 1984 *J. Appl. Phys.* **55** 3479
[14] Barandiarán J M, Gorria P, Orúe I, Fernández-Gubieda M L, Plazaola F, Gómez Sal J C, Fernández Barquín L and Fournes L 1997 *J. Phys.: Condens. Matter* **9** 5671
[15] Michalsen C and Schultz L 1991 *Acta Metall. Mater* **39** 987
[16] Czjzek G, Fink J, Götz F, Schmidt H, Coey J M D, Rebouillat J P and Liénard A 1981 *Phys. Rev.* B **23** 2513
[17] Le Caër G and Brand R A 1998 *J. Phys.: Condens. Matter* **10** 10 715
[18] Varret F and Henry M 1980 *Revue Phys. Appl.* **15** 1057
[19] López Herrera M E, Grenèche J M and Varret F 1983 *Phys. Rev.* B **28** 4944
[20] Panissod P, Durand J and Budnick J I 1982 *Nucl. Instrum. Methods* **199** 99
[21] Zhang Jianqiang, Wu Bingyao, Wu Xiaohua, Wang Guiqin and Zhao Jiwan 1996 *J. Appl. Phys.* **79** 5473
[22] Garitaonandia J S, Barandiarán J M, Gorria P and Righi L 1998 *Mater. Sci. Forum* **269–272** 431
[23] Garitaonandia J S, Righi L, Barandiarán J M, Gorria P, Leccabue F and Watts B E 1997 *Mater. Sci. Forum* **235–238** 193
[24] Barandiaran J M, Gorria P, Orue I, Fernández-Gubieda M L, Plazaola F and Hernando A 1996 *Phys. Rev.* B **54** 3026
[25] Garitaonandia J S, Schmool D S and Barandiarán J M 1998 *Phys. Rev.* B **58** 12 147